

Relaxation and nonradiative decay in disordered systems. II. Two-fracton inelastic scattering

S. Alexander,* Ora Entin-Wohlman,[†] and R. Orbach

Department of Physics, University of California, Los Angeles, California 90024

(Received 1 April 1985; revised manuscript received 19 November 1985)

The two localized-vibrational quanta (Raman) relaxation process is calculated for a localized electronic state. The calculation is expected to be relevant to relaxation at elevated temperatures where the principal vibrational excitations are of high energy (and hence of short length scale). Localization of the vibrational eigenstates is most likely for this regime. Vibrational localization can be geometrical in origin (as on a fractal network, with the quantized vibrational states fractons), or as a consequence of scattering (analogous to Anderson localization, with the quantized vibrational states localized phonons). The relaxation rate is characterized by a probability density which is calculated for both classes of localization under the assumption that the electronic and vibrational energy widths are larger than the maximum electronic relaxation rate. The time profile of the initial electronic state population is calculated. The long-time behavior begins as $t^{1/2(a-1)}\exp[-c_1(t)^{1/(a-1)}]$, where $a = 4q + 2\bar{d}$ and $4q + 2\bar{d} - 2$ for Kramers and non-Kramers transitions, respectively. Here, \bar{d} is the fracton dimensionality and $q = \bar{d}d_\phi/D$. The fractal dimensionality is D , and d_ϕ is defined by the range dependence of the fracton wave function: $\phi \propto \exp(-r^{d_\phi})$. The long-time behavior thus begins as a stretched exponential. After a crossover time, the long-time behavior varies as $(\ln t)^{\eta-1/2}t^{-c_1(\ln t)^{2\eta}}$ where c_1 is a constant and $\eta = D/d_\phi$. This portion of the time decay is faster than any power law but slower than exponential or stretched exponential. In the presence of rapid electronic cross relaxation, the time profile is exponential, with a low-temperature relaxation time $1/T_1^{\text{ve}}$ proportional to $T^{-2\bar{d}[1+2(d_\phi/D)]-1}$ and $T^{-2\bar{d}[1+2(d_\phi/D)]-3}$ for Kramers and non-Kramers transitions, respectively. These results may explain recent fractional temperature exponents found for electronic spin-lattice relaxation in macromolecules and nuclear spin-lattice relaxation in glasses.

I. INTRODUCTION

There has been considerable recent interest in the dynamical properties of random systems.¹ Experiments by Stapleton *et al.*² were the first to suggest that spin-lattice relaxation processes in macromolecules could be attributed to the fractal character of the molecular structure. Their results exhibited a fractional temperature dependence for the Raman spin-lattice relaxation rate. They related this dependence to a density of vibrational states which was specified by the fractal dimension D (which gives the range dependence of the atomic density) of the macromolecule as determined from an x-ray scattering analysis of the atomic positions within the macromolecule. Their analysis, however, did not take into account the range dependence of the force constant acting between constituents of the macromolecule.³ It was shown by Alexander and Orbach³ that when this was done, a new dimension, the so-called fracton dimension \bar{d} , was necessary to account for the density of vibrational states.

It is tempting to simply insert \bar{d} for D in the original expressions of Stapleton *et al.*,² but this would be incorrect. For, in addition to the density of vibrational states depending on a different parameter, one must also consider the localization of the vibrational states.⁴ As we shall show in this paper, this profoundly affects the spin-lattice relaxation rate, both in terms of its temporal characteristics and its temperature dependence.

The purpose of this paper is to calculate the two-vibration contribution to the spin-lattice relaxation time of localized magnetic centers (e.g., electronic or nuclear moments) in structures where the vibrational states are localized. There is some reason to believe that this calculation may be relevant to other materials as well as macromolecules. Previous work has suggested that glasses and other amorphous materials may exhibit fracton vibrational excitations at high energies.⁵ Indeed, Thorpe⁶ and He and Thorpe⁷ interpret the elastic properties of covalent glasses in terms of an amorphous solid in which rigid regions percolate. This would represent a condition where the mass density is Euclidean (i.e., $D = d$), but where, because of the percolating character of the bonding, $\bar{d} \leq d$. Other examples would be hydrated gels, where a similar separation between mass density and force-constant behavior obtains (the former Euclidean, the latter fractal) epoxy resins⁸ and particle aggregates.⁹

As Stapleton *et al.* show,² the observation of noninteger exponents for the temperature dependence of the spin-lattice relaxation rate can itself serve as an indication that the material host exhibits fractal vibrational excitations. Our perspective is similar. We explore the time and temperature dependence for spin-lattice relaxation of localized centers in disordered hosts. Our predictions can then be used to determine the character of the vibrational excitations in such materials.

We have argued that at very long length scales all materials will behave as Euclidean structures.³ It is only for

the short-length-scale vibrational excitations that one can expect localization, and under some circumstances, fractal geometry. We separate the long- from the short-length-scale regime by a characteristic length scale ξ . We denote vibrational excitations with wavelength $\lambda \geq \xi$ as phonons. Those with characteristic lengths $\leq \xi$ are referred to as fractons, or localized phonons, depending on whether the geometry is fractal, or Euclidean, respectively. We show below that the latter is a special case of the former, so that it is more general to work with fractons at short length scales.

We denote the vibrational frequency corresponding to the characteristic length scale ξ by ω_c , the so-called cross-over frequency. For a fractal network, on which the diffusion constant scales with length as $D(r) \propto r^{-\theta}$,¹⁰ $\omega_c \propto \xi^{-[1+(\theta/2)]}$. For localized phonons (Euclidean geometry), $\theta=0$ and one is concerned with the usual localization edge in the Anderson sense¹¹ at $\lambda \approx \xi$.

Clearly, the detailed behavior in the length-scale region near ξ will be complex. Because ξ corresponds to an energy scale ω_c , we address ourselves to the spin-lattice relaxation rate at temperatures such that the thermally excited vibrational states have energies substantially in excess in $\hbar\omega_c$. Thus, we work "deep" in the fracton regime where the asymptotic form of Alexander and Orbach³ for the density of vibrational states is accurate.

It will prove fruitful to make reference to the percolating network when we actually evaluate our expressions. Though such a structure is clearly only a model, it is one which is quite illustrative and for which nearly all of the parameters which enter into our treatment have been calculated. Here, the characteristic length ξ is just the percolation correlation length ξ_p . Our calculation, being relevant to high temperatures, thereby depends on vibrational excitations whose characteristic length scale is much smaller than ξ_p . Those excitations of length scale comparable to and longer than ξ_p will not contribute significantly to the high-temperature Raman relaxation process (exactly similar behavior is found for Euclidean structures and is the reason why the two-phonon Raman process dominates the one-phonon direct process at high temperatures¹²).

Our treatment in this paper will take into account not only the alteration of the vibrational density of states caused by fractal geometry, but, as noted above, also the localization of the vibrational states inherent for a fractal network with $\bar{d} \leq 2$,⁴ or for a Euclidean network with sufficient impurity scattering.¹¹ This feature will manifest itself directly in the time dependence of the magnetization. The relaxation rate at various electronic sites will differ because of fluctuations in the spatial location of suitable nearby vibrational levels. This will lead to a broad distribution of relaxation rates and to a time dependence for the initial electronic level occupation which is different from the usual exponential law found for extended vibrational modes.

In previous papers^{13,14} we considered the relaxation of an excited localized electronic state interacting with a single localized vibrational mode (the one-quantum process). The primary assumption of our model was that the energy-dependent localization length of the vibrational

modes, l_ω , was the only length scale in the problem (because we worked deep in the fracton regime, at length scales $\ll \xi$). We distinguished between two types of localized vibrational states: (i) fractons, localized because of the fractal geometry of the vibrating network, and (ii) localized phonons, localized in the Anderson sense because of static imperfection scattering. These two types of localization were characterized by differing energy dependences of their respective localization lengths, and by their differences in density of states. As a result, the matrix element of the electron-vibration interaction exhibited different energy dependences for the two cases. We then derived the probability density for the relaxation rate for both classes of vibrational states and used it to obtain the time dependence of the population of the initial electronic state. In both situations, we found that the decay at long times was characterized by the law $t^{-(\ln t)^x}$, where t is the time measured in suitable units and the exponent x is determined by the dimensionalities describing the underlying network. Thus, the long-time decay due to one-fracton or one-phonon emission has the same functional form. The only difference lies in the expression for the exponent x .

We consider in this paper the relaxation of a localized electronic state caused by the absorption and subsequent emission of two-vibrational modes, the difference in vibrational energies equaling the change in electronic energy. We obtain in this manner an explicit expression for the spin-lattice relaxation time in the Raman regime for a paramagnetic impurity in a disordered system. A preliminary version of this theory has already appeared.¹⁵

A difference between one- and two-vibrational relaxation will show up in this paper. The fracton and localized phonon cases will exhibit different temporal decays for two-vibration-induced relaxation. The difference will arise from the difference in energy dependences of the localization lengths assumed for the two cases.

The ordinary (extended-phonon) Raman relaxation process utilizes primarily phonons of high energy (a few multiples of $k_B T$) because it depends upon the integral of the square of the density of states multiplied by positive powers of the phonon frequency. In this paper, we shall assume that the localization length of the localized phonon states is energy independent. The strength of the Raman relaxation process will then also depend upon the higher-energy vibrational modes, just as for extended phonon states. The only difference is the broad distribution of relaxation rates obtained for localized phonons. It is this broad distribution which will lead to the peculiar decay rate described above.

The fracton Raman relaxation process will differ from the localized phonon Raman relaxation process because of the energy dependence of the fracton localization length. In general, this length will decrease as the fracton energy increases. Thus, the probability that a given localized electronic site has two fractons in its vicinity capable of inelastic scattering will increase as the frequency of each fracton decreases. Our subsequent treatment will show that, when $\beta\omega_c < 1$, the fracton Raman process is dominated by the lower-energy fracton modes. This, in combination with the distribution of relaxation rates caused

by fracton localization, will lead to a decay in the time domain of a stretched exponential form. This is not true for the localized phonon Raman relaxation process under the conditions assumed in this paper: the decay will always be of the form $t^{-(\ln t)^x}$, though x will depend on the specific time domain.

We shall study in Sec. III the two-fracton Raman relaxation process. We first derive the probability density for the largest relaxation rate seen at a given localized electronic state site. The Laplace transform of this probability density then generates the time dependence of the electronic return to equilibrium. We find that, at long times, the return to equilibrium will begin as a stretched exponential, afterwards crossing over to an $e^{-(\ln t)^x}$ law. We calculate the average relaxation rate from the first moment of the probability density and compare it with Stapleton's calculation,² which did not take fracton localization into account.

The calculation of the two-fracton Raman relaxation process is extraordinarily complex. As a consequence, we shall sketch, in Sec. II of this paper, the procedure we shall follow in subsequent sections. The principal results of our paper are derived in Sec. III. The reader who is only interested in the results may omit Sec. III and pass directly to the Summary (Sec. V) where a comparison is made between the conclusions of this paper and previous work. Section IV contains a development similar to Sec. III, but for localized phonons. Its results are also included in the Summary.

II. GUIDE TO THE CALCULATION

The problem faced when calculating the two-fracton relaxation process arises principally from the localization of the vibrational wave functions. The localized electronic sites are embedded in a "sea" of fractons, of all energies $\hbar\omega_\alpha$ and concomitant length scales l_{ω_α} . We take the fractons localized,⁴ so that different electronic sites will interact with different sets of fractons. Thus, even though the overall fracton-excitation-energy density of states is smoothly varying with fracton energy, the spectrum of fractons interacting with a particular electronic site will not vary smoothly with fracton energy (i.e., as the fracton energy changes, the spatial position of the higher-energy fractons will vary randomly). Such is not the case for extended phonons, where all localized electronic sites couple equally strongly with a particular vibrational state.

As a consequence, each electronic site will experience a different fracton-induced Raman relaxation rate. That is, the relaxation rate W for the full electronic system will be described by a probability density $P(W)$. The principal problem addressed in this paper is the calculation of $P(W)$.

We do so by making an assumption which we have proven to be valid in Ref. 15. We calculate the transition probability per unit time, $\mathcal{W}(\omega_\alpha, L, L')$, for a particular electronic site to relax upon the absorption of a fracton of energy $\hbar\omega_\alpha$ centered a distance L away from the electronic site, and the emission of a fracton of energy $\omega_\alpha + \omega_0$ centered a distance L' away from the electronic site, with ω_0 being the change in electronic energy. We shall subse-

quently ignore ω_0 in comparison with ω_α because we are interested in electronic transitions of energy $\hbar\omega_0 \ll \hbar\omega_c$, and fracton energies are (always) greater than $\hbar\omega_c$.⁵ Only ω_α will enter into our expressions for W .

The assumption we make is that the full probability density for W , $\bar{P}(W)$, is sufficiently skewed that it is sufficient to calculate only the probability density $P(W)$ for the largest relaxation rate seen by a given electronic site. This may seem surprising at first, but our (unpublished) calculations have shown that, for the two-fracton Raman relaxation process, the contributions to W which arise from W smaller than the largest [i.e., from summing $\mathcal{W}(\omega_\alpha, L, L')$ over L and L' , for L, L' larger than the closest value] generate only logarithmic corrections to W . We have shown this explicitly for the one-fracton relaxation process in an Appendix to Ref. 14. Length considerations prevent our doing so here for the two-fracton relaxation process.

The probability density for the *largest* relaxation rate experienced by an electronic site is denoted by $P(W)$. Remarkably, we are able to obtain a closed-form expression for $P(W)$, and to evaluate it analytically at small W .

The calculation proceeds as follows. We calculate $\mathcal{W}(\omega_\alpha, L, L')$ using standard methods,¹² exhibiting the result in Eq. (3). We let $\bar{P}(W)$ be the probability that a given site experiences a relaxation rate W . Then the probability $P(W)$ that W is the largest relaxation rate for that site is given by $\bar{P}(W)$ multiplied by the probability that no other W will be larger. This can be collapsed to the form of Eq. (7):

$$P(W) = \bar{P}(W) \exp \left[- \int_W^{W_{\max}} dW' \bar{P}(W') \right],$$

where W_{\max} is the relaxation rate for $L = L' = 0$, i.e., for both fractons centered on the electronic site.

To find $\bar{P}(W)$, we take $\mathcal{W}(\omega_\alpha, L, L')$ and multiply by (i) [Eq. (8)] the probability of finding a fracton within a distance L , $L + dL$ from the electronic site, with energy between ω_α and $\omega_\alpha + d\omega_\alpha$; (ii) [Eq. (10)] the same probability for the second fracton at L' ; and (iii) the energy-conserving delta function. Integrating over ω_α , L , and L' then gives us $\bar{P}(W)$ [Eq. (11)].

The remainder of the calculation for $P(W)$ is complex and tedious, with explicit forms for $P(W)$ at small W exhibited in Eq. (26). It is a straightforward process to calculate the time decay profile $P(t)$, the occupation of the initial electronic state, by taking the Laplace transform of $P(W)$. The results are exhibited in Eqs. (28) and (29).

These calculations have all assumed that the electronic states do not communicate with one another, i.e., that they relax independently. The presence of couplings between the electronic sites (e.g., dipolar or exchange spin-spin couplings) can tie the individual site magnetizations to one another if sufficiently strong. This "cross relaxation" then causes the electronic system to relax as a whole, with a single decay rate equal to the average relaxation rate $\langle W \rangle \equiv 1/T_1^{\text{ave}}$. The time decay profile is then a simple exponential, quite different from that obtained for independent electronic site relaxation.

We calculate $1/T_1^{\text{ave}}$ both by taking the first moment of $P(W)$ and by direct calculation. The temperature depen-

dence, given by Eq. (33), differs substantially from the conventional result for electronic relaxation caused by extended phonons.

Section IV, the calculation of the localized phonon Raman process, follows closely the methods of Sec. III. The time decay profile is found to be of the same analytic form as the very-long-time two-fracton result [$P(t) \propto t^{-(\ln t)^2}$]. The temperature dependence of $1/T_1^{\text{ave}}$ is exactly the same as for extended phonons. This guide to Secs. III and IV should enable the interested reader to follow the complex algebraic calculations contained therein.

III. THE TWO-FRACTON RAMAN PROCESS

We calculate the two-fracton relaxation rate for a Kramers doublet. The two fractons are located at distances L and L' , respectively, from the center of the localized electronic site. The energy difference between the electronic ground doublet and an excited doublet (in order to break time-reversal symmetry) is Δ , and the Zeeman-energy splitting of the ground doublet is ω_0 . The matrix element of the interaction with the vibrational modes for short-range forces is proportional to the strain components of the local medium. We expand the distortion of the surrounding medium in terms of fracton normal modes. The wave function for the α th fracton mode with energy ω_α is assumed to have the form

$$\phi_\alpha(\omega_\alpha) \propto (l_{\omega_\alpha})^{-D/2} \exp\left[-\frac{1}{2}(L/l_{\omega_\alpha})^{d_\phi}\right], \quad (1)$$

where l_{ω_α} is the localization length. Here, D is the Hausdorff dimension of the fractal. We expect the localization of the vibrational wave function to scale with the Pythagorean length L as exhibited in Eq. (1). Under some conditions,¹⁶ d_ϕ may be replaced by d_{\min} , where $l \propto L^{d_{\min}}$, such that l is the shortest path between two points separated by a Pythagorean distance L .¹⁷ Whether such an identification holds for fractal networks in general is somewhat controversial. One should therefore regard Eq. (1) as a trial wave function of sufficient generality that appropriate identification of d_ϕ will allow all of our subsequent results to be applied to specific physical situations. The interaction matrix element is proportional to the spatial derivative of the fracton wave function, and thence to $(l_{\omega_\alpha})^{-d_\phi}$. Using the energy dependence of the fracton localization length,⁵

$$l_{\omega_\alpha} \propto \omega_\alpha^{-\bar{d}/D}, \quad (2)$$

where \bar{d} is the fracton dimensionality;³ we find that the spatial derivative of ϕ_α is proportional to ω_α^q where $q = \bar{d}(d_\phi/D)$.

The Raman relaxation rate involves an absorption (emission) of a vibrational mode of energy ω_α and an emission (absorption) of a vibrational mode of energy $\omega_\alpha + \omega_0$. In general, ω_α will be of the order of thermal energies. Hence, $\omega_\alpha \gg \omega_0$. The overall rate is proportional to the fourth power of the interaction matrix element (because both vibrations enter the expression for the transition probability per unit time). Putting all these elements together, the relaxation rate is proportional to

$$W(\omega_\alpha, L, L') \propto \left\{ (l_{\omega_\alpha})^{-2D} \omega_\alpha^{4q-2} \right. \\ \left. \times \exp\left[-(L/l_{\omega_\alpha})^{d_\phi} - (L'/l_{\omega_\alpha})^{d_\phi}\right] \right\} \\ \times \left[\frac{e^{\beta\omega_\alpha}}{(e^{\beta\omega_\alpha} - 1)^2} \right] \frac{1}{\delta(\omega_\alpha, L, L')} \frac{\omega_\alpha^2}{\Delta^4}. \quad (3)$$

The terms in the curly brackets result from the square of the matrix element (ω_α^{-2} arises from the normal-mode expansion). The terms in the large parentheses are the vibration occupation numbers. The factor $\delta(\omega_\alpha, L, L')$ represents the combined widths of the electronic and fracton vibrational states. Here, $1/\delta(\omega_\alpha, L, L')$ replaces the energy-conserving delta function which usually appears in the golden rule formula for extended vibrational states. The factor $(\omega_\alpha/\Delta^2)^2$ appears in the relaxation rate of Kramers doublets and arises from the dynamical breaking of the time-reversed symmetry of the ground doublet.¹² For non-Kramers transitions, it is replaced by $(1/\Delta)^2$. We rewrite Eq. (3) in the form

$$W(\omega_\alpha, L, L') = W_m(\omega_\alpha) \frac{\delta(\omega_\alpha, 0, 0)}{\delta(\omega_\alpha, L, L')} \\ \times \exp\left[-(L/l_{\omega_\alpha})^{d_\phi} - (L'/l_{\omega_\alpha})^{d_\phi}\right]. \quad (4)$$

where,

$$W_m(\omega_\alpha) = W_0 \beta^{-a} (\beta\omega_\alpha)^a e^{\beta\omega_\alpha} / (e^{\beta\omega_\alpha} - 1)^2. \quad (5)$$

Here,

$$a = \begin{cases} 4q + 2\bar{d}, & \text{Kramers transitions} \\ 4q + 2\bar{d} - 2, & \text{non-Kramers transitions} \end{cases} \quad (6)$$

W_0 is a constant divided by $\delta(\omega_\alpha, 0, 0)$ and $\beta = 1/k_B T$. When $a > 2$, $W_m(\omega_\alpha)$ is peaked at a certain value of $\beta\omega_\alpha$ (this value is zero for $a = 2$). We denote the maximal value of $W_m(\omega_\alpha)$ by W_{\max} .

We next construct the probability density $P(W)$ for the largest relaxation rate seen at a given spin site. This consists of the probability density $\bar{P}(W)$ for a given relaxation rate W times the probability that no relaxation rate is larger than W :

$$P(W) = \bar{P}(W) e^{-F(W)}, \quad (7a)$$

with

$$F(W) = \int_W^{W_{\max}} dW' \bar{P}(W'). \quad (7b)$$

The probability density $\bar{P}(W)$ consists of three factors: (i) the probability of finding a fracton state within a distance L , $L + dL$, of the localized electronic site, with energy between ω_α and $\omega_\alpha + d\omega_\alpha$:

$$N_{\text{fr}}(\omega_\alpha) DL^{D-1} dL d\omega_\alpha, \quad (8)$$

where $N_{\text{fr}}(\omega_\alpha)$ is the fracton density of states (per atomic volume),

$$N_{\text{fr}}(\omega_\alpha) = \bar{d} \omega_\alpha^{\bar{d}-1} / \Omega_f^{\bar{d}}, \quad (9)$$

and Ω_f is the fracton Debye frequency;⁵ (ii) the probability of finding a second fracton state at distance $L', L' + dL'$ from the electronic site with energy between

ω_α and $\omega_\alpha + \delta(\omega_\alpha, L, L')$ is given by

$$N_{\text{fr}}(\omega_\alpha) D(L')^{D-1} dL' \delta(\omega_\alpha, L, L'); \quad (10)$$

(iii) a delta function requiring the relaxation rate $W(\omega_\alpha, L, L')$ to be equal to W . Thus,

$$\begin{aligned} \bar{P}(W) = \int d\omega_\alpha \int dL \int dL' D^2 L^{D-1} (L')^{D-1} \delta(\omega_\alpha, L, L') \\ \times N_{\text{fr}}^2(\omega_\alpha) \delta(W(\omega_\alpha, L, L') - W). \end{aligned} \quad (11)$$

In order to carry out the calculation of the probability density $P(W)$, Eq. (7a), from $\bar{P}(W)$, Eq. (11), we need to specify the distance and energy dependence of the combined electronic and fracton energy widths $\delta(\omega_\alpha, L, L')$. We consider two limits for the one-fracton relaxation problem previously:^{13,14} (i) rapid fracton relaxation or rapid cross relaxation for the electronic state, whence $\delta(\omega_\alpha, L, L')$ is a constant, independent of ω_α , L , or L' , and (ii) slow fracton relaxation and negligible electronic cross relaxation, whence $\delta(\omega_\alpha, L, L')$ is replaced by the relaxation rate W itself. The latter requires a self-consistent solution for $P(W)$ which, for the two-fracton case, is prohibitively complex. The former allows for a straightforward, though by no means simple, treatment. We therefore treat the former limit and replace

$$\delta(\omega_\alpha, L, L') = \delta(\omega_\alpha, 0, 0) = \delta. \quad (12)$$

We insert Eqs. (4) and (11) into Eq. (7b) and find (see Appendix A for details)

$$F(W) = \eta B(\eta, \eta + 1) \delta I(\beta, W), \quad (13)$$

where

$$\begin{aligned} I(\beta, W) = \int d\omega_\alpha [N_{\text{fr}}(\omega_\alpha) l_{\omega_\alpha}^D]^2 \{ \ln [W_m(\omega_\alpha) / W] \}^{2\eta} \\ \times \Theta(W_m(\omega_\alpha) - W), \end{aligned} \quad (14)$$

with

$$\eta = D/d_\phi. \quad (15)$$

$\Theta(x)$ is the unit step function and $B(\eta, \eta + 1)$ is the beta function (here, just a numerical constant).

The ω_α integration in Eq. (14) is confined to the region where $W_m(\omega_\alpha) \geq W$. From Eq. (5) for $W_m(\omega_\alpha)$, we find that this region is bounded from below by ω_1 and from above by ω_2 , where ω_1 and ω_2 are the solutions of

$$W/W_1 = (\beta\omega_\alpha)^a e^{\beta\omega_\alpha} / (e^{\beta\omega_\alpha} - 1)^2, \quad (16)$$

with

$$W_1 = W_0 \beta^{-a}. \quad (17)$$

[Note that the function on the right-hand side of Eq. (16)

is double valued as long as $a > 2$. This is obeyed for exponents appropriate to most fractals (see below.) However, there are further limitations on the physically accessible values of ω_α . The fracton energies are bounded from above by the fracton Debye energy Ω_f and from below by a cutoff energy. This is either the crossover frequency separating the extended phonon (low-frequency) regime from the fracton (high-frequency) regime, or the Zeeman energy ω_0 , whichever is larger. Denoting the lower cutoff frequency by ω_c , one has to replace ω_1 by ω_c whenever $\omega_1 < \omega_c$ and ω_2 by Ω_f whenever $\omega_2 > \Omega_f$.

We now use the relationship

$$N_{\text{fr}}(\omega_\alpha) l_{\omega_\alpha}^D = \bar{d} / \omega_\alpha \quad (18)$$

to write $I(W)$ [Eq. (14)] in the form

$$I(W) = (\bar{d})^2 \beta \int_{z_1}^{z_2} dz \frac{1}{z^2} \left[\ln \left[\frac{W_1}{W} \right] + \ln \left[\frac{z^a e^z}{(e^z - 1)^2} \right] \right]^{2\eta}, \quad (19)$$

where the $z_{1,2} = \beta\omega_{1,2}$ specify the integration limits as discussed above. Note the factor z^{-2} in Eq. (19). This gives great weight to the region of small z in the integrand. It results from the relation between the energy dependence of the localization length and the fracton density of states [Eq. (18)]. For the extended-phonon Raman process, the density of states is alone in the integrand and weighs most heavily the larger frequency regime (until the $k_B T$ limit imposed by the Bose factor). In the fracton Raman process, the energy dependence of the localization length l_{ω_α} shifts the weight in the integrand to the smaller frequency regime.

The function $I(W)$ is a monotonically decreasing function of W . As W approaches W_{max} it tends to zero:

$$I(W) \propto [1 - (W/W_{\text{max}})]^{2\eta+1/2}, \quad 1 - (W/W_{\text{max}}) \ll 1. \quad (20)$$

because in this case the integration region is very small. For W/W_1 values ≤ 1 , the integral in Eq. (19) is dominated by the contributions of the small- z region. In the small- z limit, the solution of Eq. (16) with $\beta\omega_\alpha = z$ is

$$z_1 = (W/W_1)^{1/(a-2)}, \quad a > 2. \quad (21)$$

Therefore, for $W < W_1(\beta\omega_c)^{a-2}$, the lower bound of the integration is $\beta\omega_c$, provided that $\beta\omega_c < 1$. For $W > W_1(\beta\omega_c)^{a-2}$, the lower bound is z_1 , as given by Eq. (21). Denoting

$$W_c = W_1(\beta\omega_c)^{a-2}, \quad (22)$$

we find that the contribution to $I(W)$ arising from the small- z region is

$$I(W) = \begin{cases} (\bar{d})^2 \beta (a-2)^{2\eta} (W_1/W)^{1/(a-2)} \left[\Gamma(2\eta+1) - \Gamma \left[2\eta+1, \frac{1}{a-2} \ln(W_1 z_0^{a-2}/W) \right] \right], & W > W_c \\ (\bar{d})^2 \beta (a-2)^{2\eta} (W_1/W)^{1/(a-2)} \left[\Gamma \left[2\eta+1, \frac{1}{a-2} \ln(W_c/W) \right] - \Gamma \left[2\eta+1, \frac{1}{a-2} \ln(W_1 z_0^{a-2}/W) \right] \right], & W < W_c. \end{cases} \quad (23a)$$

$$W < W_c. \quad (23b)$$

Here, $\Gamma(x)$ and $\Gamma(x,y)$ are the complete and incomplete gamma functions, respectively, and z_0 is a number of order unity. For small values of W/W_1 the limiting behaviors of Eqs. (23) are

$$I(W) \sim \begin{cases} (\bar{d})^2 \beta (a-2)^{2\eta} \Gamma(2\eta+1) \beta (W_1/W)^{1/(a-2)}, & W > W_c \\ (\bar{d})^2 \beta (a-2)^{2\eta} \beta (W_1/W)^{1/(a-2)} \Gamma \left[2\eta+1, \frac{1}{a-2} \ln(W_c/W) \right], & W < W_c \end{cases} \quad (24a)$$

$$I(W) \sim \begin{cases} (\bar{d})^2 \beta (a-2)^{2\eta} \beta (W_1/W)^{1/(a-2)} \Gamma \left[2\eta+1, \frac{1}{a-2} \ln(W_c/W) \right], & W < W_c \\ (\bar{d})^2 (1/\omega_c) [\ln(W_c/W)]^{2\eta}, & W \ll W_c. \end{cases} \quad (24b)$$

$$I(W) \sim \begin{cases} (\bar{d})^2 \beta (a-2)^{2\eta} \beta (W_1/W)^{1/(a-2)} \Gamma \left[2\eta+1, \frac{1}{a-2} \ln(W_c/W) \right], & W < W_c \\ (\bar{d})^2 (1/\omega_c) [\ln(W_c/W)]^{2\eta}, & W \ll W_c. \end{cases} \quad (24b')$$

The expression (24b') results from the limit $W \ll W_c$ of the incomplete gamma function, where we have also used Eq. (22).

Figure 1 portrays $I(W)$ versus W/W_1 as computed directly from Eq. (19) (curve *a*) and from the approximated expressions, Eqs. (23) (curve *b*). The difference between the two curves is rather small. One notes that the contribution of the large- z region to $I(W)$, for small values of W/W_1 , is of the order of $\beta(\ln(W_1/W))^{2\eta}$. When $\beta\omega_c < 1$, this is smaller by a factor of $\beta\omega_c$ than the contribution of the small- z region for $W < W_c$ [see Eq. (24b)]. We shall adopt, therefore, Eq. (23) and their limiting forms, Eqs. (24), in subsequent calculations.

We now return to the probability density $P(W)$ for the largest relaxation rate seen at a given site [Eq. (7a)] and use it to find the time dependence of the population of the initial electronic state. The time profile is found by taking the Laplace transform of the probability density

$$P(t) = \int_0^{W_{\max}} dW P(W) e^{-Wt}. \quad (25)$$

We consider the decay of the initial population at long times. We need, therefore, the probability density at small values of W/W_1 [W_1 being of the order of W_{\max}]. See the discussion after Eq. (6)]. Using Eqs. (24) in Eqs. (7) and (13), we find

$$P_1(W) dW = \alpha_1 \beta \delta \frac{1}{a-2} (W_1/W)^{1/(a-2)} \times \exp\{-\alpha_1(\beta\delta)(W_1/W)^{1/(a-2)}\} dW/W, \quad W > W_c, \quad (26a)$$

$$P_2(W) dW = \alpha_2 (\delta/\omega_c) 2\eta [\ln(W_c/W)]^{2\eta-1} \times \exp\{-\alpha_2(\delta/\omega_c) [\ln(W_c/W)]^{2\eta}\} dW/W, \quad W \ll W_c, \quad (26b)$$

where α_1 and α_2 are the numerical constants

$$\alpha_1 = \eta B(\eta, \eta+1) (\bar{d})^2 (a-2)^{2\eta} \Gamma(2\eta+1)$$

and

$$\alpha_2 = \eta B(\eta, \eta+1) (\bar{d})^2,$$

respectively. The integral in Eq. (25) is separated accordingly into two terms:

$$P(t) \sim \int_{W_c}^{W_1} P_1(W) e^{-Wt} dt + \int_0^{W_c} P_2(W) e^{-Wt} dt. \quad (27)$$

We carry out the integrations by the saddle-point method

(the details are given in Appendix B). The contribution of the first term in Eq. (27) to $P(t)$ is

$$P_1(t) \sim (t/t_1)^{1/2(a-1)} \exp[-\alpha_3(t/t_1)^{1/(a-1)}], \quad t < t_1 (\delta/\omega_c)^{a-1}, \quad (28a)$$

where the time constant t_1 is

$$t_1 = [\alpha_1/(a-2)] (1/W_1) (1/\beta\delta)^{a-2} \quad (28b)$$

and α_3 is the numerical constant $\alpha_3 = \alpha_1(a-1)/(a-2)$. The contribution of the second term in Eq. (27) is

$$P_2(t) \sim (\delta/\omega_c)^{1/2} [\ln(t/t_2)]^{\eta-1/2} \times \exp\{-\alpha_2(\delta/\omega_c) [\ln(t/t_2)]^{2\eta}\}, \quad t > t_2, \quad (29a)$$

where the time constant t_2 is

$$t_2 = (2\eta\alpha_2/W_c) (\delta/\omega_c). \quad (29b)$$

From these equations, we see that the long-time behavior of $P(t)$ begins as a stretched exponential [Eq. (28a)]. The temperature dependence of the time constant t_1 (assuming that the level width δ is temperature independent) is found from Eqs. (17) and (28b): $t_1 \sim \beta^2$. At a time of the order $t_1(\delta/\omega_c)^{a-1}$, the decay changes its character. From Eq. (29a), it is seen that it is slower than the stretched exponential but faster than a power law. In this regime, the time constant is proportional to $(\beta\delta)^2(\omega_c)^{1-a}$, using Eqs.

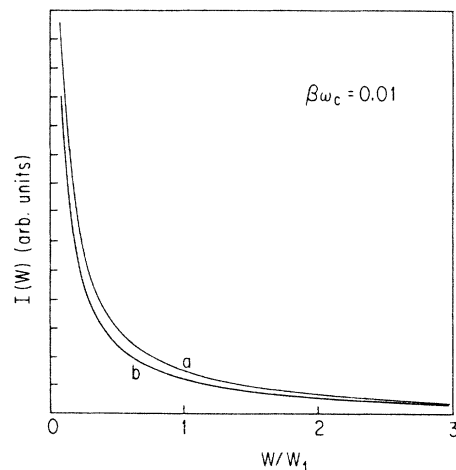


FIG. 1. Function $I(W)$ computed from Eq. (19) (curve *a*) and from the approximate forms Eq. (23) (curve *b*). The parameters used are $\beta\omega_c = 0.01$, $\beta\Omega_f = 6.0$, $a = 5.63$, and $\eta = 1.8$ (appropriate to a percolating network for $d_\phi = d_{\min}$).

(17), (22), and (29b) and the relationship [Eq. (5)] $W_0 \propto \delta^{-1}$. The peculiar time behavior exhibited by Eq. (29a) is similar to the one found^{13,14} for the relaxation of a localized electronic level by virtue of the one-fracton process. It results from the $[\ln(W_c/W)]^{2\eta}$ dependence of $F(W)$.

As the temperature is lowered and $\beta\omega_c$ increases, the small- z region of the integrand in Eq. (19) gradually diminishes in importance. Then, for small values of W/W_1 the leading behavior of $I(W)$ is given by $\beta(\ln(W_1/W))^{2\eta}$. This is identical to the behavior exhibited by Eq. (24b'), with ω_c and W_c replaced there by $1/\beta$ and W_1 , respectively. Consequently, the behavior of $P(t)$ at long times and in the limit $\beta\omega_c > 1$ is given by Eqs. (29a) (with $\omega_c \rightarrow \beta^{-1}$, $W_c \rightarrow W_1$) and is thus slower than exponential.

We now consider the situation where the magnetic moments of the relaxing levels are strongly cross relaxing. The levels then relax at the average of the probability density for the relaxation rate. The return to equilibrium is expected to be exponential. Denoting the average relaxation rate by $1/T_1^{\text{ave}}$, we evaluate it by taking the first moment of the probability density for W :

$$1/T_1^{\text{ave}} = \int_0^{W_{\text{max}}} dW WP(W). \quad (30)$$

We use the approximate expressions, Eqs. (26), for $P(W)$. Because the integral in Eq. (30) includes W , we may neglect the contribution of $P_2(W)$ [see Eq. (26b)] to Eq. (30) and use instead only the part pertaining to the larger values of $W/W_1, P_1(W)$ as given by Eq. (26a). This approximation becomes better as $\beta\omega_c$ becomes smaller (i.e., as the temperature increases) because W_c is then much smaller than W_1 [see Eq. (22)]. Inserting Eq. (26a) into Eq. (30) and substituting $x = (W_1/W)^{1/(a-2)}$, we find

$$1/T_1^{\text{ave}} = \alpha_1 \beta \delta W_1 \int_1^{(W_1/W_c)^{1/(a-2)}} dx e^{-\alpha_1 \beta \delta x} x^{2-a}. \quad (31)$$

For $a > 3$, the integral is dominated by its lower bound; for $2 < a < 3$, it is dominated by the upper bound. As a result,

$$1/T_1^{\text{ave}} \sim \begin{cases} W_1 \beta \delta, & a > 3 \\ W_1 \beta \delta (1/\beta\omega_c)^{3-a}, & 3 > a > 2, \end{cases} \quad (32)$$

where we have used Eq. (22). It turns out that, for percolating networks with $d_\phi = d_{\text{min}}$, $a > 3$ both for Kramers and non-Kramers transitions. For general d_ϕ with $a > 3$, one has

$$1/T_1^{\text{ave}} \sim \begin{cases} T^{2\bar{d}[1+2(d_\phi/D)]-1}, & \text{Kramers transitions} \\ T^{2\bar{d}[1+2(d_\phi/D)]-3}, & \text{non-Kramers transitions.} \end{cases} \quad (33)$$

The results of Eq. (32) can be derived directly by averaging over the relaxation rate seen at given spin site [Eqs. (4) and (5)]. We carry out this procedure explicitly. Consider a volume of radial distance L around the spin site. The fraction of pairs of fracton states whose wave functions are localized within this volume is $(l_{\omega_\alpha}/L)^{2D}$. The number of fracton states with energies in the range $\omega_\alpha, \omega_\alpha + d\omega_\alpha$ is $N_{\text{fr}}(\omega_\alpha)L^D d\omega_\alpha$. Similarly, the number of fracton states with energy in the range $\omega_\alpha, \omega_\alpha + \delta$ (where δ

is the combined electron and fracton energy widths) is $N_{\text{fr}}(\omega_\alpha)L^D \delta$. Therefore, the fraction of fracton-state pairs which dominate the relaxation process is

$$[N_{\text{fr}}(\omega_\alpha)l_{\omega_\alpha}^D]^2 \delta d\omega_\alpha \exp[-N_{\text{fr}}(\omega_\alpha)l_{\omega_\alpha}^D \delta], \quad (34)$$

where the exponential insures that the second fracton state of the pair is the closest available to the first fracton member of the pair. We multiply Eq. (34) by the relaxation rate $W_m(\omega_\alpha)$ [Eq. (5)] for the pair at energy ω_α and integrate over all energies to find

$$1/T_1^{\text{ave}} = \int_{\omega_c}^{\Omega_f} d\omega_\alpha [N_{\text{fr}}(\omega_\alpha)l_{\omega_\alpha}^D]^2 \times \delta \exp[-N_{\text{fr}}(\omega_\alpha)l_{\omega_\alpha}^D \delta] W_m(\omega_\alpha). \quad (35)$$

Using the relation Eq. (18) between the fracton density of states and the localization length, and substituting $\beta\omega_\alpha = 1/x$, Eq. (35) takes the form

$$1/T_1^{\text{ave}} = W_1 \beta \delta (\bar{d})^2 \int_1^{1/\beta\omega_c} dx e^{-\bar{d}\beta\delta x} x^{2-a}. \quad (36)$$

Here we have used the small $\beta\omega_\alpha$ expansion of the fracton occupation numbers [see Eq. (5)] and, correspondingly, the lower bound of the x integration has been taken to be of the order of 1. Equation (36) has the same form as Eq. (31) and therefore leads to the same expressions for $1/T_1^{\text{ave}}$ as Eqs. (32). Note that W_1 is proportional to $1/\delta$ [see Eq. (17) and the discussion after Eq. (6)]. Hence, the average relaxation rate is independent of δ .

The explicit temperature dependence of $1/T_1^{\text{ave}}$ is T^{a-1} for $a > 3$ and T^2 for $2 < a < 3$. This result differs from that of Stapleton *et al.*,² in that they did not include the energy dependence of the localization length for fractons. As a consequence, their result is limited to $q=1$, so that they obtain $a=4+2\bar{d}$ for Kramers transitions and $a=2+2\bar{d}$ for non-Kramers transitions. In order to evaluate our expressions explicitly, we set $d_\phi = d_{\text{min}}$. This is probably an overestimate (i.e., we expect $d_\phi \leq d_{\text{min}}$). In three dimensions, we then find for percolating networks $q \sim 0.74$ ($q = \bar{d}d_{\text{min}}/D$, $\bar{d} = \frac{4}{3}$, and $D/d_{\text{min}} = 1.8$). Hence, from Eq. (6), $a=5.63$ for Kramers transitions and 3.63 for non-Kramers transitions. Using Eq. (33), this leads to

$$1/T_1^{\text{ave}} \sim \begin{cases} T^{4.63} & \text{for Kramers transitions} \\ T^{2.63} & \text{for non-Kramers transitions,} \end{cases} \quad (37)$$

respectively.

IV. THE LOCALIZED PHONON RAMAN PROCESS

We now reduce the results of the preceding section to the limit of phonons localized in the Anderson sense (i.e., as a result of impurity scattering). We refer to the geometry of this condition as Euclidean, implying that $d_\phi = 1$ (and $\bar{d} = D = d$, so that $q = 1$). We ignore effects of a localization edge by neglecting any energy dependence of the localization length $l_{\omega_\alpha} \equiv \xi$. We take the localized phonons to obey a linear dispersion law and we set the spatial derivative of the localized phonon eigenstates proportional to their energy. These simplifications can all be relaxed under specific conditions, but we make them here

in order to illustrate the principal differences between relaxation by fractons and localized phonons.

Making the above replacements in Eqs. (3), (4), and (5) results in the same form for relaxation as for the fracton Raman process. [Note that the factor $2\bar{d}$ in Eq. (6) results from the energy dependence of the fracton localization length.] The only difference is that the value of the energy exponent a changes to

$$a_{\text{ph}} = \begin{cases} 4, & \text{Kramers transitions} \\ 2, & \text{non-Kramers transitions.} \end{cases} \quad (38)$$

When $a_{\text{ph}}=2$, the maximum value of $W_m(\omega_\alpha)$ [Eq. (5)] is located at $\omega_\alpha=0$, and $W_m(\omega_\alpha)$ is a single-valued function.

$$I(W) = d^2(\xi/\beta\Omega_{\text{ph}})^{2d}\beta \int_{z_1}^{z_2} dz z^{2d-2} [\ln(W_1/W) + \ln(z^{a_{\text{ph}}}e^z/(e^z-1)^2)]^{2d}. \quad (40)$$

Here,

$$W_1 = W_0\beta^{-a_{\text{ph}}} \quad (41)$$

and $z_{1,2}$ are the solutions of Eq. (16) (with a replaced by a_{ph}) for $a_{\text{ph}}=4$. For $a_{\text{ph}}=2$, $z_1=0$. Again, for $z_2 > \beta\Omega_{\text{ph}}$, z_2 is replaced by $\beta\Omega_{\text{ph}}$, and for $z_1 < \beta\omega_c$, z_1 is replaced by $\beta\omega_c$ where ω_c is the lower cutoff frequency (localization edge) for the localized phonons.

As opposed to the two-fracton case, the principal contribution to the z integration for $I(W)$ [Eq. (40)] arises from the large- z region (i.e., for higher energies). The reason lies with the density-of-states weighting factor in Eq. (40): z^{2d-2} . This shifts the weight to the large- z regime. For fractons, the energy dependence of the localization length changes this factor to z^{-2} . Thus, the principal distinction between the contribution of fractons versus localized phonons to the Raman relaxation process lies in the energy region which contributes principally to $I(W)$, leading to a difference in form for the probability density $P(W)$.

The function $I(W)$, Eq. (40), is monotonically decreasing with W . For W close to W_{max} , it attains the form of Eq. (20) with η replaced by d . For small values of W/W_1 and $\beta\Omega_{\text{ph}} > 1$, the contribution of the large- z region to $I(W)$ is

$$I(W) \sim \begin{cases} [\gamma_1/(2d-1)][\ln(W_1/W)]^{4d-1}, & \ln(W_1/W) < \beta\Omega_{\text{ph}} \\ [\gamma_1/(2d-1)](\beta\Omega_{\text{ph}})^{2d-1}[\ln(W_1/W)]^{2d}, & \ln(W_1/W) > \beta\Omega_{\text{ph}}, \end{cases} \quad (42a)$$

$$\quad (42b)$$

where

$$\gamma_1 = d^2(\xi/\beta\Omega_{\text{ph}})^{2d}\beta. \quad (43)$$

Following exactly the same procedures as in Sec. III, we obtain the probability density $P(W)$ (for small W/W_1 and $\beta\Omega_{\text{ph}} > 1$) for localized phonons, to be compared with

The same philosophy obtains for the derivation for the probability density for the largest relaxation rate seen at a given site for localized phonons as for fractons. Therefore, we can use Eqs. (13) and (14), replacing $l_{\omega_\alpha}^D$ by ξ^d and η [see Eq. (15)] by the embedding dimensionality d . The localized phonon density of states (see list of assumptions above) is taken equal to

$$N_{\text{ph}}(\omega_\alpha) = d\omega_\alpha^{d-1}/\Omega_{\text{ph}}^d, \quad (39)$$

where Ω_{ph} is the phonon Debye frequency. Because the phonon localization length ξ has been taken to be energy independent, the function $I(W)$, as defined by Eq. (14), takes the form

Eqs. (26) for fractons:

$$P_1(W)dW = \gamma_2(4d-1)[\ln(W_1/W)]^{4d-2} \times \exp\{-\gamma_2[\ln(W_1/W)]^{4d-1}\}dW/W, \quad \ln(W_1/W) < \beta\Omega_{\text{ph}}, \quad (44a)$$

where,

$$\gamma_2 = [d^3/(2d-1)] \frac{(d-1)d!}{(2d)!} (\xi/\beta\Omega_{\text{ph}})^{2d}\beta\delta, \quad (44b)$$

and

$$P_2(W)dW = \gamma_3 2d[\ln(W_1/W)]^{2d-1} \times \exp\{-\gamma_3[\ln(W_1/W)]^{2d}\}dW/W, \quad \ln(W_1/W) > \beta\Omega_{\text{ph}}, \quad (45a)$$

where

$$\gamma_3 = \gamma_2(\beta\Omega_{\text{ph}})^{2d-1}. \quad (45b)$$

Inserting the expressions in Eqs. (44) and (45) in Eq. (25), we obtain the time profile for the initial electronic state population after time t . The details of the calculations are given in Appendix C. The results are

$$P_1(t) \sim (\gamma_2)^{1/2} [\ln(t/t_1)]^{2d-1} \times \exp\{-\gamma_2[\ln(t/t_1)]^{4d-1}\}, \quad t_1 < t < t_1 e^{\beta\Omega_{\text{ph}}}, \quad (46a)$$

where the characteristic time t_1 is

$$t_1 = \gamma_2(4d-1)/W_1, \quad (46b)$$

and

$$P_2(t) \sim (\gamma_3)^{1/2} [\ln(t/t_2)]^{d-1/2} \times \exp\{-\gamma_3[\ln(t/t_2)]^{2d}\}, \quad t > t_2 e^{\beta\Omega_{\text{ph}}}, \quad (47a)$$

where the characteristic time t_2 is

$$t_2 = \gamma_3 2d / W_1 . \quad (47b)$$

The long-time behavior of $P(t)$ [Eqs. (46a) and (47a)] at low temperatures ($\beta\Omega_{\text{ph}} > 1$) is slower than exponential but faster than any power law. At shorter times, the decay is rather rapid, with the characteristic time t_1 increasing with increasing temperature for $d=3$ [From Eqs. (41), (44b), and (46b), $t_1 \propto T^{2d-1-a_{\text{ph}}}$]. At longer times, the decay becomes slower, with the characteristic time t_2 decreasing with increasing temperature [From Eqs. (41), (44b), (45b), and (47b), $t_2 \propto T^{-a_{\text{ph}}}$]. In both regimes the time decay obeys a law of the form $e^{-(\ln t)^x}$. The same time dependence has been found for one-vibrational quantum relaxation.¹ For that process, both fracton and localized phonon relaxation yield the same time dependence. For two-vibrational quanta relaxation, the difference in the energy dependence of the localization lengths between fractons and localized phonons manifests itself through different time dependences [Eqs. (28a) and (46a)] characterizing the beginning of the long-time behavior.

We next calculate the average response time for two-localized-phonon (Raman) relaxation. This would be appropriate for rapid cross relaxation between the electronic sites. We calculate the first moment of the probability densities Eqs. (44) and (45) and then integrate over W to obtain the contribution of localized phonons to the average spin-lattice relaxation rate, $1/T_1^{\text{ave}}$, at low temperatures. Inserting Eqs. (44) and (45) into Eq. (30), we find

$$1/T_1^{\text{ave}} \sim \gamma_2 W_1 \int_0^{(\beta\Omega_{\text{ph}})^{4d-1}} dx e^{-\gamma_2 x} e^{-x^{1/(4d-1)}} + \gamma_3 W_1 \int_{(\beta\Omega_{\text{ph}})^{2d}}^{\infty} dx e^{-\gamma_3 x} e^{-x^{1/2d}} . \quad (48)$$

Here, we have substituted $x = [\ln(W_1/W)]^{4d-1}$ to obtain the first term in Eq. (48), and $x = [\ln(W_1/W)]^{2d}$ to obtain the second. In the limit $\beta\Omega_{\text{ph}} > 1$, the second member of Eq. (48) may be neglected. The first is of the order of $\gamma_2 W_1$. Consequently, using Eqs. (41) and (44b),

$$1/T_1^{\text{ave}} \sim \begin{cases} T^{3+2d}, & \text{Kramers transitions} \\ T^{1+2d}, & \text{non-Kramers transitions} . \end{cases} \quad (49)$$

This result reproduces the normal (low-temperature) temperature dependence for extended phonons for the Raman relaxation process.

Finally, we consider the high-temperature limit, $\beta\Omega_{\text{ph}} < 1$. Returning to Eq. (40), we find that in this limit

$$I(W) \sim \begin{cases} d^2 \xi^{2d} (1/\Omega_{\text{ph}}) \{ \ln[(W_1/W)(\beta\Omega_{\text{ph}})^2] \}^{2d} , \\ a_{\text{ph}} = 4 \\ d^2 \xi^{2d} (1/\Omega_{\text{ph}}) [\ln(W_1/W)]^{2d} , \\ a_{\text{ph}} = 2 . \end{cases} \quad (50)$$

Taking into account that $W_1 \propto \beta^{-a_{\text{ph}}}$ [Eq. (41)], we see that $I(W)$ has the same form and temperature dependence for both Kramers ($a_{\text{ph}}=4$) and non-Kramers ($a_{\text{ph}}=2$) transitions. The probability density $P(W)$ pertaining to the high-temperature limit is

$$P(W)dW = \gamma_4 (\delta/\Omega_{\text{ph}}) 2d [\ln(\tilde{W}/W)]^{2d-1} \times \exp\{-\gamma_4 (\delta/\Omega_{\text{ph}}) [\ln(\tilde{W}/W)]^{2d}\} , \quad (51)$$

where γ_4 is a constant independent of the temperature,

$$\gamma_4 = d^3 \frac{(d-1)! d!}{(2d)!} \xi^{2d} , \quad (52)$$

and $\tilde{W} \sim W_0 \beta^{-2}$ [see Eqs. (50)]. The long-time behavior of the initial electronic state population is given by

$$P(t) \sim (\gamma_4 \delta/\Omega_{\text{ph}})^{1/2} [\ln(t/\tilde{\tau})]^{d-1/2} \times \exp\{-\gamma_4 (\delta/\Omega_{\text{ph}}) [\ln(t/\tilde{\tau})]^{2d}\} , \quad (53)$$

with the characteristic time given by

$$\tilde{\tau} = \gamma_4 (\delta/l_{\text{ph}}) / \tilde{W} \sim \beta^2 , \quad (54)$$

which increases as the temperature decreases. The first moment of the distribution Eq. (51) is of the order of \tilde{W} . Thus, at low temperature, $1/T_1^{\text{ave}} \sim T^2$, both for Kramers and non-Kramers transitions. This again reproduces the normal (high-temperature) temperature dependence for extended phonons for the Raman relaxation process.

V. SUMMARY AND CONCLUSIONS

We have shown how localization of vibrational excitations can profoundly affect the relaxation of localized electronic states. We have calculated the distribution of relaxation rates for the condition that the combined energy widths of the electronic and vibrational states exceed the maximum relaxation rate W_{max} and are temperature independent. This is appropriate to rapid anharmonic relaxation of the vibrational states, for example.

We have calculated the probability density for the largest relaxation rate, as seen from a particular electronic site. For two-fracton relaxation, the near-long-time profile for the probability of remaining in the initial electronic state is a "stretched exponential":

$$P_1(t) \propto \exp[-\alpha_3 (t/t_1)^{1/(a-1)}] \quad (\text{two fractons}) , \quad (28')$$

where α_3 is a numerical constant, t_1 is a characteristic time, and $a = 4q + 2\bar{d}$ for Kramers transitions and $a = 4q + 2\bar{d} - 2$ for non-Kramers transitions, respectively. Here, $q = \bar{d}(d_\phi/D)$. For the far-long-time profile, one finds

$$P_2(t) \propto t^{-[\ln(t/t_2)]^{2\eta}} \quad (\text{two fractons}) , \quad (29')$$

where t_2 is another characteristic time and $\eta = D/d_\phi$. For the case of localized phonons, the near-long-time profile takes the form

$$P_1(t) \propto t^{-[\ln(t/t'_1)]^{4d-1}} \quad (\text{localized phonons}) , \quad (46')$$

where t'_1 is a characteristic time. For the far-long-time profile, one finds

$$P_2(t) \propto t^{-[\ln(t/t'_2)]^{2d}} \quad (\text{localized phonons}) , \quad (47')$$

where t'_2 is another characteristic time.

Under the assumption of rapid electronic cross relaxation, the time profile becomes a simple exponential, with a

characteristic relaxation rate equal to the first moment of the distribution $P(W)$. We find the following temperature dependences for the average spin-lattice relaxation rates.

Two-fracton Raman relaxation:

$$1/T_1^{\text{ave}} \propto \begin{cases} T^{2\bar{d}[1+2(d_\phi/D)]-1}, & \text{Kramers transitions} \\ T^{2\bar{d}[1+2(d_\phi/D)]-3}, & \text{non-Kramers transitions.} \end{cases} \quad (33')$$

Extended or localized two-phonon Raman relaxation:

$$1/T_1^{\text{ave}} \propto \begin{cases} T^{3+2d}, & \text{Kramers transitions} \\ T^{1+2d}, & \text{non-Kramers transitions.} \end{cases} \quad (49')$$

If we set $d_\phi = d_{\min}$ and evaluate Eq. (33) for a percolating network in $d=3$, we find the following.

Two-fracton Raman relaxation:

$$1/T_1^{\text{ave}} \propto \begin{cases} T^{4.63}, & \text{Kramers transitions} \\ T^{2.63}, & \text{non-Kramers transitions,} \end{cases} \quad (37')$$

to be compared to the following.

Extended or localized two-phonon Raman relaxation:

$$1/T_1^{\text{ave}} \propto \begin{cases} T^9, & \text{Kramers transitions} \\ T^7, & \text{non-Kramers transitions.} \end{cases} \quad (49'')$$

We see that the exponent of the temperature dependence for $1/T_1^{\text{ave}}$ is much smaller for two-fracton versus two-phonon Raman relaxation. Such low powers have been observed¹⁸ for nuclear quadrupolar relaxation in glasses (i.e., non-Kramers transitions), but were attributed to interactions with two-level systems. A two-fracton interpretation may be more relevant, but independent values for the parameters entering into Eq. (33) need to be obtained from thermal and neutron diffraction measurements.^{19,20}

ACKNOWLEDGMENTS

This research was supported under National Science Foundation Grant No. DMR-84-12898, and by the fund for basic research administered by the Israel Academy of Sciences and Humanities.

APPENDIX A: DERIVATION OF EQS. (13) AND (14)

We evaluate the integral

$$F(W) = \int_W^{W_{\max}} dW' \bar{P}(W'), \quad (A1)$$

with $\bar{P}(W)$ given by Eq. (11). The delta function appearing in Eq. (11) requires that the contribution to the integral arise from the region

$$W \leq W_m(\omega_\alpha, L, L') \leq W_{\max}, \quad (A2)$$

where $W_m(\omega_\alpha, L, L')$ is given by Eq. (4). Clearly, the right inequality is always satisfied. Therefore, we need only consider the region of W appropriate to the left inequality. We define

$$A(W, \omega_\alpha) = \ln[W_m(\omega_\alpha)/W]. \quad (A3)$$

Then,

$$F(W) = \delta \int d\omega_\alpha [N_{\text{fr}}(\omega_\alpha) l_{\omega_\alpha}^D]^2 \times \int d(x^\eta) d[(x')^\eta] \Theta(A-x-x') \Theta(A), \quad (A4)$$

where we have used Eq. (12). Here, $\eta = D/d_\phi$ and $\Theta(x)$ is the unit step function. Carrying out the x and x' integrations, we find

$$F(W) = \eta B(\eta, \eta+1) \delta \int d\omega_\alpha [N_{\text{fr}}(\omega_\alpha) l_{\omega_\alpha}^D]^2 \times [A(W, \omega_\alpha)]^{2\eta} \Theta(A(W, \omega_\alpha)), \quad (A5)$$

where $B(\eta, \eta+1)$ is the beta function,

$$B(\eta, \eta+1) = \int_0^1 dy y^{\eta-1} (1-y)^\eta. \quad (A6)$$

Equations (A3) and (A5) together give Eqs. (13) and (14) directly.

APPENDIX B: DERIVATION OF EQS. (28) AND (29)

We carry out the integrations in Eq. (27) by the saddle-point method. Inserting Eq.(26a) into the first term of Eq. (27) and denoting

$$x = (W_1/W)^{1/(a-2)}, \quad (B1)$$

we find

$$P_1(t) = \int_1^{(W_1/W_c)^{1/(a-2)}} dx \alpha_1 \beta \delta \exp(-\alpha_1 \beta \delta x - W_1 t x^{2-a}), \quad (B2)$$

where α_1 is a numerical constant (see text). The limiting behavior of $P_1(t)$ is found by the saddle-point method. The saddle point x_0 of the integrand in Eq. (B2) is

$$x_0 = [(a-2)W_1 t / \alpha_1 \beta \delta]^{1/(a-1)} \quad (B3)$$

and, consequently,

$$P_1(t) \sim [2\pi\alpha_1\beta\delta/(a-1)]^{1/2} \left[\frac{(a-2)W_1 t}{\alpha_1\beta\delta} \right]^{1/2(a-1)} \times \exp \left[-\frac{a-1}{a-2} \alpha_1\beta\delta \left[\frac{(a-2)W_1 t}{\alpha_1\beta\delta} \right]^{1/(a-1)} \right] \quad (B4)$$

One notes that the condition for the saddle point to lie within the integration bounds, $x_0^{2-a} < W_1/W_c$, is equivalent to

$$(a-2)W_1 t / \alpha_1 < \beta\delta / (\beta\omega_c)^{a-1}, \quad (B5)$$

where we have used Eq. (22). The stretched exponential decay exhibited in Eq. (B4) exhibits the characteristic time t_1 ,

$$t_1 = [\alpha_1/(a-2)] \frac{1}{W_1} (\beta\delta)^{2-a}. \quad (B6)$$

Equation (B4) is valid for times such that $t < t_1(\delta/\omega_c)^{a-1}$.

Inserting Eq. (26b) into the second term of the right-hand side of Eq. (27) and substituting

$$x = [\ln(W_c/W)]^{2\eta}, \quad (\text{B7})$$

we find

$$P_2(t) = \int_0^\infty dx \alpha_2(\delta/\omega_c) \times \exp[-\alpha_2(\delta/\omega_c)x - W_c t e^{-x^{1/2\eta}}], \quad (\text{B8})$$

where α_2 is a numerical constant (see text). The saddle point x_0 obeys the equation

$$t e^{-x_0^{1/2\eta}} x_0^{(1/2\eta)-1} = t_2, \quad (\text{B9})$$

where we have introduced

$$t_2 = (2\eta\alpha_2/W_c)(\delta/\omega_c). \quad (\text{B10})$$

At times such that $t < t_2$, the leading order solution of Eq. (B9) is $x_0 = (t/t_2)^{2\eta/(2\eta-1)}$. Consequently, the leading behavior of $P_2(t)$ is exponential: $P_2(t) \sim \exp(-W_c t)$, $t < t_2$. Because $t_2 \sim t_1(\delta/\omega_c)^{a-1}$ [from Eqs. (22), (B6), and (B10)], the exponential behavior of $P_2(t)$ falls in the time region where Eq. (B5) is valid. In this region, the time profile is dominated by $P_1(t)$ [Eq. (B4)], which decays slower than exponential. At times such that $t > t_2$, the leading order solution of Eq. (B9) is

$$x_0 \sim [\ln(t/t_2)]^{2\eta}, \quad (\text{B11})$$

and the leading behavior of $P_2(t)$ is

$$P_2(t) \sim (4\pi\eta\alpha_2\delta/\omega_c)^{1/2} [\ln(t/t_2)]^{\eta-1/2} \times \exp\{-\alpha_2(\delta/\omega_c)[\ln(t/t_2)]^{2\eta}\}, \quad t > t_2. \quad (\text{B12})$$

APPENDIX C: DERIVATION OF EQS. (44) AND (45)

The Laplace transform of the probability density given by Eqs. (44) and (45) is

$$P(t) = P_1(t) + P_2(t), \quad (\text{C1})$$

where

$$P_1(t) = \int_0^{(\beta\Omega_{\text{ph}})^{4d-1}} dx \gamma_2 \exp(-\gamma_2 x - W_1 t e^{-x^{1/(4d-1)}}) \quad (\text{C2})$$

and

$$P_2(t) = \int_{(\beta\Omega_{\text{ph}})^{2d}}^\infty dx \gamma_3 \exp(-\gamma_3 x - W_1 t e^{-x^{1/2d}}). \quad (\text{C3})$$

To obtain the first member of $P(t)$, $P_1(t)$, we have substituted

$$x = [\ln(W_1/W)]^{4d-1}$$

into Eq. (44a). Similarly, the substitution

$$x = [\ln(W_1/W)]^{2d}$$

into Eq. (45a) generates $P_2(t)$.

We use the saddle-point method to find the long-time behavior of $P(t)$. The saddle point x_0 of the integrand in Eq. (C2) obeys the equation

$$t_1 = t x_0^{(2-4d)/(4d-1)} e^{-x_0^{1/(4d-1)}}, \quad (\text{C4})$$

where the characteristic time t_1 is given by

$$t_1 = \gamma_2 [(4d-1)/W_1]. \quad (\text{C5})$$

For $t < t_1$, the solution of Eq. (C4) is

$$x_0 = (t/t_1)^{(4d-1)/(4d-2)},$$

and the leading behavior of $P_1(t)$ is exponential. For $t > t_1$, the solution of Eq. (C4), to leading order, is

$$x_0 \sim [\ln(t/t_1)]^{4d-1}. \quad (\text{C6})$$

Integrating around the saddle point, we obtain

$$P_1(t) \sim [2\pi(4d-1)\gamma_2]^{1/2} [\ln(t/t_1)]^{2d-1} \times \exp\{-\gamma_2 [\ln(t/t_1)]^{4d-1}\}, \quad t_1 < t < t_1 e^{\beta\Omega_{\text{ph}}}, \quad (\text{C7})$$

where the requirement that $t < t_1 e^{\beta\Omega_{\text{ph}}}$ insures that the saddle-point Eq. (C6) is within the integration limits.

The saddle point of the integrand in Eq. (C3) is given by the equation

$$t_2 = t x_0^{(1-2d)/2d} e^{-x_0^{1/2d}}, \quad (\text{C8})$$

with $t_2 = \gamma_3(2d/W_1)$. In this case, there is no solution for $t < t_2$ [because the lower bound of the integral in Eq. (C3) is greater than unity]. For $t > t_2 e^{\beta\Omega_{\text{ph}}}$, the leading behavior of $P_2(t)$ is

$$P_2(t) \sim (4\pi d \gamma_3)^{1/2} [\ln(t/t_2)]^{d-1/2} \times \exp\{-\gamma_3 [\ln(t/t_2)]^{2d}\}. \quad (\text{C9})$$

*Permanent address: The Racah Institute, The Hebrew University, Jerusalem, Israel.

† Permanent address: School of Physics and Astronomy, Tel Aviv University, Ramat Aviv, 69978 Tel Aviv, Israel.

¹See, in its entirety, *J. Stat. Phys.* **36** (1985); see also *Proceedings of the NATO Advanced Study Institute, Geilo, Norway* (Plenum, New York, 1985).

²H. J. Stapleton, J. P. Allen, C. P. Flynn, D. G. Stinson, and S.

Kurtz, *Phys. Rev. Lett.* **45**, 1456 (1980); J. P. Allen, J. T. Colvin, D. G. Stinson, C. P. Flynn, and H. J. Stapleton, *Biophys. J.* **38**, 299 (1982).

³S. Alexander and R. Orbach, *J. Phys. (Paris) Lett.* **43**, L625 (1982).

⁴R. Rammal and G. Toulouse, *J. Phys. (Paris) Lett.* **44**, L13 (1983).

⁵S. Alexander, C. Laermans, R. Orbach, and H. M. Rosenberg,

- Phys. Rev. B **28**, 4615 (1983).
- ⁶M. F. Thorpe, *J. Non-Cryst. Solids* **57**, 3155 (1983).
- ⁷H. He and M. F. Thorpe, *Phys. Rev. Lett.* **54**, 2107 (1985).
- ⁸H. M. Rosenberg, *Phys. Rev. Lett.* **54**, 704 (1985).
- ⁹S. K. Sinha, T. Freltoft, and J. Kjems, *Kinetics of Aggregation and Gelation*, edited by F. Family and D. P. Landau (Elsevier Science, New York, 1984), p. 87.
- ¹⁰Y. Gefen, A. Aharony, and S. Alexander, *Phys. Rev. Lett.* **50**, 77 (1983).
- ¹¹S. John, H. Sompolinsky, and M. J. Stephen, *Phys. Rev. B* **27**, 5592 (1983).
- ¹²R. Orbach and H. Stapleton, *Electronic Paramagnetic Resonance*, edited by S. Geschwind (Plenum, New York, 1972), p. 121.
- ¹³S. Alexander, Ora Entin-Wohlman, and R. Orbach, *J. Phys. (Paris) Lett.* **46**, L549 (1985).
- ¹⁴S. Alexander, Ora Entin-Wohlman, and R. Orbach, *Phys. Rev. B* **32**, 6447 (1985).
- ¹⁵S. Alexander, Ora Entin-Wohlman, and R. Orbach, *J. Phys. (Paris) Lett.* **46**, L555 (1985).
- ¹⁶Y.-E. Levy and B. Souillard (unpublished).
- ¹⁷K. M. Middlemiss, S. G. Whittington, and D. S. Gaunt, *J. Phys. A* **13**, 1835 (1980); R. Pike and H. E. Stanley, *ibid.* **14**, L169 (1981); D. C. Hong and H. E. Stanley *ibid.* **16**, L475 (1983); **16**, L525 (1983); H. J. Herman, D. C. Hong, and H. E. Stanley, *ibid.* **17**, L261 (1984); J. Vannimenus, J. P. Nodal, and C. Martin, *ibid.* **17**, L351 (1984); S. Havlin and R. Nossal, *ibid.* **17**, L427 (1984); S. Havlin, Z. V. Djordjevic, I. Majid, H. E. Stanley, and G. H. Weiss, *Phys. Rev. Lett.* **53**, 178 (1984).
- ¹⁸J. Szeftal and H. Alloul, *Phys. Rev. Lett.* **34**, 657 (1975); *J. Non-Cryst. Solids* **29**, 253 (1978).
- ¹⁹R. C. Zeller and R. O. Pohl, *Phys. Rev. B* **4**, 2029 (1971).
- ²⁰U. Buchenau, N. Nucker, and A. J. Dianoux, *Phys. Rev. Lett.* **53**, 2316 (1984); P. F. Tua, S. Putterman, and R. Orbach (unpublished).